IEEE Access
Multidisciplinary : Rapid Review : Open Access Journal

Received October 3, 2021, accepted November 14, 2021, date of publication November 16, 2021, date of current version December 2, 2021.

Digital Object Identifier 10.1109/ACCESS.2021.3128583

Design and Optimization of a Hybrid Excitation System for Magnetically Driven Rotating DC Arc Plasma Generators

XIAOWEN XU[1], ZHUOXIANG REN[2], (Senior Member, IEEE), AND SHIYOU YANG[1], (Senior Member, IEEE)
[1]College of Electrical Engineering, Zhejiang University, Hangzhou 310027, China
[2]Laboratory of Electronics and Electromagnetism, Sorbonne Universités, Université Pierre et Marie Curie, 75005 Paris, France

Corresponding author: Shiyou Yang (eesyyang@zju.edu.cn)

This work was supported in part by the National Key Research and Development Program Subject of China under Grant 2016YFB0301804.

ABSTRACT To eliminate the disadvantages of both the uncontrollability in the magnetic field of a permanent magnet excitation system and the high energy consumption of an electric excitation system in a traditional magnetically rotating arc plasma generator, a novel topology of a hybrid permanent magnet and electrically excited coil system is proposed. The proposed system will generate a large enough magnetic field to drive the arc rotation with a minimum consumption of materials and electric energy in the normal operation duty, and will guarantee a nearly zero magnetic field in the arc triggering stage. To optimize the hybrid excitation system, a comprehensive analysis and an optimization methodology; by combining finite element analysis, the moving the least squares approximation and an adaptive weighted particle swarm optimization, are proposed. Finally, a prototype hybrid excitation system is optimized with promising results in views of both saving a huge amount of electric power consumptions and ensuring a nearly zero magnetic field in the arc triggering.

INDEX TERMS Design optimization, hybrid excitation, particle swarm optimization, plasma devices, response surface methodology.

I. INTRODUCTION

In a coaxial dc arc plasma generator, the arc burns between the inside a cylindrical electrode and a rod cathode or between the cylindrical concentric electrodes [1], [2]. In order to reduce the electrode erosion, the arc attachment is forced to rotate. This is implemented by imposing an axial magnetic field. The Lorentz force acted on the arc current by this magnetic field drives the rotation of the arc column. The arc root will move along a circular path to spread the heat load [3]. To generate the constant axial magnetic field, either an electrically excited field winding [4] or a permanent magnet excitation system [5] is used.

In the developments of an electrically excited field winding system, different efforts are reported. The cathode attachment behaviors in a magnetically rotating arc plasma generator were investigated in [6]. Based on thermodynamic simulations, the effect of the input power, the feed rate and the working gas flow rate on the pyrolysis performance were systematically studied in [7]. Attempts are also devoted to further reduce the erosion of the device. For example, a method to further reduce electrode erosion by applying an external circumferential magnetic field was proposed in [3] and [8]. In these existing works, the axial magnetic field is generally produced by the coaxial electrode coils [9]. However, an electrically excited coil system will consume an enormous electric energy. Moreover, the electric power consumed by such electrically excited coil systems will become unbearable with an increasing demand for engineering coaxial dc arc plasma generators. Consequently, it is necessary to explore an energy saving excitation system for coaxial dc arc plasma generators.

In the development of a permanent magnet excitation system for coaxial dc arc plasma generators, a few work is reported [5], [10]. A silent disadvantage of such an excitation system is the difficulty to trigger an arc due to a strong

The associate editor coordinating the review of this manuscript and approving it for publication was Diego Oliva.

Lorentz force. As a result, a permanent magnet excitation system is rarely applied in engineering.

To develop an energy saving and feasible magnetic field system for a coaxial dc arc plasma generator, a hybrid excitation system of an electrically excited field coil and a permanent magnet is proposed in this paper. In the normal operating condition, the axial magnetic field is supplied by the permanent magnet, while in the triggering of the arc, the magnetic fields generated by the permanent magnet will be exactly cancelled out by the magnetic fields of the winding system in the proposed hybrid excitation system. However, the design of such a hybrid exciting system is not an easy task.

First, the hybrid excitation system is not a simple combination of the aforementioned two systems as explained in the next section.

Second, considering the following facts: (a) the computation of the magnetic fields by FEM is time consuming, (b) a stochastic optimal algorithm is generally required to solve the proposed design problem due to the multimodal characteristics of the objective functions, (c) a bi–level optimization is featured for the proposed design problem, and (d) a thousand of iterations or repeated calls of finite element simulations are generally required in a stochastic optimal algorithm, the optimal design of the hybrid excitation system is overwhelming computationally heavy.

It should be noted that no report on such a hybrid excitation system and its optimization procedure can be referenced. In this respect; to realize the aforementioned ultimate goals; i.e., a sufficient large axial magnetic field supplied by the permanent magnet in the normal operating condition, while the magnetic field generated by the permanent magnet is exactly cancelled out by the magnetic fields of the winding system in the triggering of the arc; of a hybrid excitation system for a coaxial dc arc plasma generator; a novel topology of the hybrid excitation system is proposed; and the comprehensive analysis and design optimization methodology are introduced in this paper.

II. A NOVEL DC ARC PLASMA GENERATOR AND ITS DESIGN OPTIMIZATION

The prototype magnetic driven arc rotating plasma generator is composed of a rod cathode, a sleeve anode, and the proposed hybrid excitation system. The schematic diagram, and the simplified two-dimensional axisymmetric model for the magnetic field computations, of the generator, are given in Fig. 1 (a) and Fig. 1 (b), respectively. This paper mainly focuses on the optimal design of the hybrid excitation system. The main challenging issues in designing the hybrid excitation system are to produce a sufficient magnetic field, say, 0.2 T, in the generator chamber using the permanent magnets under a maximum volume limitation in the normal operating condition; while to guarantee a nearly zero magnetic field in the trigging of the arc by using the electrically excited winding system to compensate exactly the magnetic field produced by the permanent magnet.

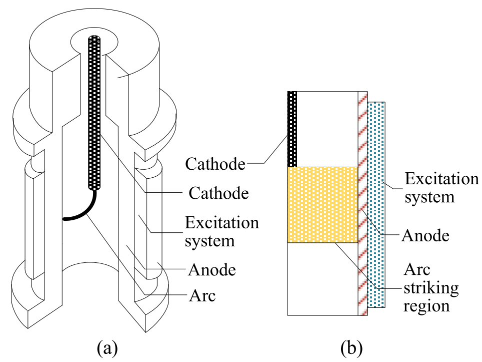

FIGURE 1. (a) Schematic diagram of the plasma generator, (b) Simplified 2D axisymmetric model for the magnetic field computation, of the plasma generator.

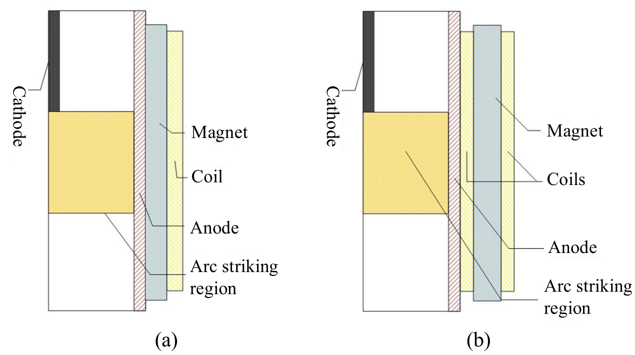

FIGURE 2. (a) Plasma generator topology with a single coil; (b) The proposed plasma generator topology with a double coil.

To develop the hybrid exciting system, one first considers a simple system topology consisted of a permanent magnet and a single electric field coil, as shown in Fig. 2 (a). Qualitatively, the variation tendency in magnetic fields produced by the single electric field coil will increase, and that of the ones produced by the permanent magnet will decrease, when the observing point approaches the anode wall. Consequently, it is very hard, even if not impossible, to guarantee a nearly zero magnetic field by using this simple hybrid excitation system in the whole region where the arc will be activated. To address this issue, a novel double coil arrangement, as shown in Figure 2 (b) and Figure 3, is proposed. The system consists of two induction coils and one permanent magnet which are coaxial with the torch body. The inner coil and the outer coil have the same shape and size, and the currents in the two coils are the same in magnitude or value but opposite in directions. The permanent magnet is a uniformly axial-magnetized cylindrical cavity which is closely located between the two coils. This topology will guarantee that the magnetic field generated by the permanent magnet will be cancelled out exactly by that of the electric coils in the arc triggering stage. Fig. 4 (a) and Fig. 4 (b) show the magnetic flux lines produced by a permanent magnet and a double coil. Obviously, the distribution profiles of the two excitation systems are nearly the same. Consequently, it is quite possible

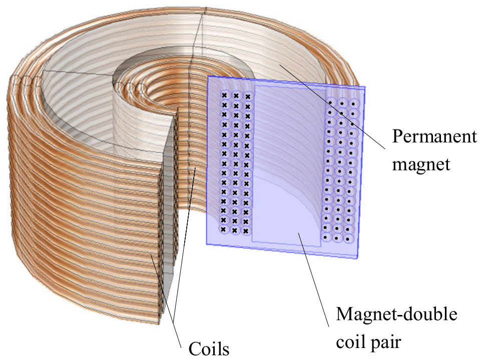

FIGURE 3. Schematic diagram of the proposed hybrid excitation system.

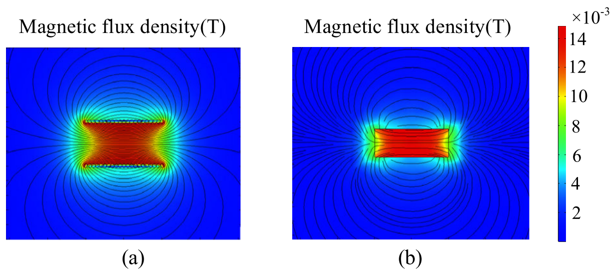

FIGURE 4. (a) Magnetic field produced by the proposed double coil system, (b) Magnetic field produced by a permanent magnet.

to produce a nearly zero magnetic field in the area of interests by imposing opposite magnetic fields from the permanent and from the proposed double coils system.

The field coils and the permanent magnets are strongly intercoupled with each other, hence they cannot be optimized separately. More specially, in order to produce a sufficient high magnetic field in the cavity under the normal operating condition, the permanent magnet design must consider the thickness of the coils; while to produce a completely uniform zero magnetic field in the triggering stage, the size of the coil and the current passing through it have a relevance with the shape of the permanent magnet. Consequently, the design of the hybrid excitation system is a bi-level optimization problem, an extremely complex and difficult problem in mathematical programming.

Considering the aforementioned intercoupled relationship, the decision variables in design optimization of the proposed hybrid excitation system include: the thickness and height of the permanent magnet, the thickness and heights of the coils, and the current density of the coils; while the objectives include minimizing the volume of the permanent magnet, ensuring the minimum magnetic field produced by the permanent magnets being large enough to exceed the required limit, and minimizing the maximum magnetic field produced by both the permanent magnets and the electrical coils in arc triggering. Mathematically, the design of the hybrid excitation system is formulated as

(1) Minimize the volume of the permanent magnet:

$$\min f_1 = \pi[(W_M + W_C + 0.15)^2 - (W_C + 0.15)^2]H_M \quad (1)$$

(2) Ensure a minimum magnetic field to be above 0.2T produced by the permanent magnet in generator chamber:

$$f_2 = B_{\min}(W_M, H_M, W_C) > 0.2\text{T} \quad (2)$$

(3) Minimize the maximum magnetic flux density in generator chamber in the arc triggering to be smaller than 0.002T:

$$f_3 = B_{\max}(W_M, H_M, W_C, H_C, J_C) < 0.002\text{T} \quad (3)$$

where W_C and H_C are, respectively, the thickness and height of the permanent magnet; W_M and H_M are, respectively, the thickness and height of the coil; J_C is the current density of the coil.

Moreover, some constraints are also applied to ensure an engineering feasibility. They include the range of the size of the permanent magnet and coils, the allowed maximum current density, i.e.,

$$\begin{cases} 0.2\text{m} < H_M < 0.6\text{m}, 0 < W_M < 0.3\text{m} \\ 0.2\text{m} < H_C < 0.6\text{m}, 0 < W_C < 0.3\text{m} \\ 0 < J_C < 20\text{A/mm}^2. \end{cases} \quad (4)$$

To solve the three-objective design optimization of the hybrid exciting system, an aggregated approach is used to transform it into a single objective function by:

$$f = f_1 \text{ for } |f_2| = 0.2 \text{ or } |f_3| = 0.002, \quad (5)$$

and

$$f = f_1 + \frac{0.1 \times \min[(|f_2| - 0.2), 0]}{|f_2| - 0.2} + \frac{0.1 \times \min[(0.002 - |f_3|), 0]}{0.002 - |f_3|} \text{ for } |f_2| \neq 0.2 \text{ and } |f_3| \neq 0.002. \quad (6)$$

III. SOLUTION METHODOLOGY

A. GENERAL SOLUTION PROCEDURE

To transfer the aforementioned constrained design problem of the proposed hybrid excitation system into an unconstrained one, the exterior penalty function method is used. To determine the magnetic field of the hybrid excitation system, a high-fidelity model, i.e., the finite element method (FEM), is used. Considering the following facts: (a) the computation of the magnetic fields by FEM is time consuming, (b) a stochastic optimal algorithm is generally required to solve the proposed design problem due to the multimodal characteristics of the objective functions, (c) a bi–level optimization is featured for the proposed design problem, and (d) a thousand of iterations or repeated calls of finite element simulations are generally required in a stochastic optimal algorithm, the optimal design of the hybrid excitation system is overwhelming computationally heavy. In these respects, a meta-model, a response surface model based on an improved moving least squares approximation, is introduced. Also, to find the global optimal solution of the multimodal objective functions of the hybrid excitation system, the adaptive weighted particle swarm optimization algorithm, a stochastic optimal algorithm proved to be effective in electromagnetic implementation and multimodal function optimization [11], [12], as reported in [13], is improved and used. To facilitate the implementation of the aforementioned methodologies, the general solution procedures for the design optimization of the proposed hybrid excitation system are given step by step as:

(1) Transfer the constrained optimization problem to an unconstrained one by using the exterior penalty function method.

(2) Discretize the decision variable space into a series of sampling points uniformly, and calculate the objective function (including the constrains) at these sampling points by FEM.

(3) Reconstruct the optimal problem by using the moving least squares approximation surface response model according to the function values on the sampling points.

(4) Apply the adaptive weighted particle swarm optimization algorithm to optimize the reconstructed optimal problem to find an approximated solution of the original design problem.

(5) Optimize the original optimization problem directly by Powell algorithm to obtain an improved solution of the optimization problem by starting from the approximated optimal solution of step 4.

(6) Compare the solutions between Steps 4 and 5. If the error is larger than a predefined value, add sampling point around the improved solution, and go to step c; otherwise, go to next step.

(7) Output the final optimal solution and the optimal function value.

To find efficiently the optimal solution of the original design problem in Step 5, a direct search method, the Powell conjugate direction method, is employed.

B. A META-MODEL BASED ON AN IMPROVED MOVING LEAST SQUARES APPROXIMATION

Response surface model or methodology (RSM) is a meta-model for replacing the true response surface by an approximate one based on the observed data at various points in the design space from the system [14]. The approximate functions used in RSMs rely mainly on multiple linear and second-order regression models [15]. The second-order model is more widely used for its flexibility [16], among which the moving least squares (MLS) regression model is one of the mostly used ones. However, in dealing with multi-dimensional problems, the existing moving least square approximation requires relatively a high density of sampling points, costing a large amount of computation times. In this regard, an improved moving least squares approximation surface response model is proposed.

1) MOVING LEAST SQUARES APPROXIMATION BASED RESPONSE SURFACE MODEL

In a MLS regression model, a number of response surfaces at their corresponding local minima are successively constructed, each approximating the true response surface over a relatively small region of the independent variable space, and the regression coefficients are fitted by least squares [17]. Considering the high variable dimension of the optimization problem, a Hermite version of MLS defined based on the design sensitivity information is used to reduce the required sample points for a sufficiently accurate approximation. To be self-contained, the Hermite MLS approximation will be briefed in this section, and a detailed explanation may be found in [18].

In general, a second-order regression model defines the local approximation function $\tilde{f}(\boldsymbol{x})$ for the true response function $f(\boldsymbol{x})$ in terms of some basis functions and some adjusting coefficients $\boldsymbol{a}$ as:

$$\tilde{f} = a_0 + \sum_{i=1}^{n} a_i x_i + \sum_{i=1}^{n} a_{ii} x_i^2 + \sum \sum_{i<j=2}^{n} a_{ij} x_i x_j = \boldsymbol{b}(\boldsymbol{x})^{\mathrm{T}} \boldsymbol{a}, \tag{7}$$

where n is the total number of independent variables and

$$\boldsymbol{b} = [1 x_1\ x_2\ \ldots\ x_n\ x_1^2\ \ldots\ x_n^2\ x_1\ x_2\ x_1\ x_3\ \ldots\ x_{n-1}\ x_n]^{\mathrm{T}}. \tag{8}$$

The Hermite MLS regression model further considers the design sensitivity information by introducing a supplementary term relative to the gradient of $f(\boldsymbol{x})$ and replaces the basis function with an expanded one, $\boldsymbol{p}(\boldsymbol{x})$, as:

$$\boldsymbol{p}(\boldsymbol{x}) = [\boldsymbol{b} \quad \frac{\partial \boldsymbol{b}}{\partial x_1} \quad \ldots \quad \frac{\partial \boldsymbol{b}}{\partial x_{\mathrm{n}}}]. \tag{9}$$

The key coefficients $\boldsymbol{a}$ are determined by a weighted least squares method by minimizing $\boldsymbol{J}(\boldsymbol{a})$, i.e., the error between the observed data and the approximated values, including that of the objective function and the derivative information. The error $\boldsymbol{J}(\boldsymbol{a})$ is defined as:

$$\boldsymbol{J}_1(\boldsymbol{a}) = \mathrm{t} \sum_{i=1}^{N} w(\|\boldsymbol{x}_i - \boldsymbol{x}\|)(\boldsymbol{p}^{\mathrm{T}}(\boldsymbol{x}_i - \boldsymbol{x})\boldsymbol{a} - f(\boldsymbol{x}_i))^2, \tag{10}$$

$$\boldsymbol{J}_2(\boldsymbol{a}) = (1-\mathrm{t}) \sum_{i=1}^{N} r_i^2 w(\|\boldsymbol{x}_i - \boldsymbol{x}\|)(\nabla \boldsymbol{p}^{\mathrm{T}}(\boldsymbol{x}_i - \boldsymbol{x})\boldsymbol{a} - \nabla f(\boldsymbol{x}_i))^2, \tag{11}$$

$$\boldsymbol{J}(\boldsymbol{a}) = \boldsymbol{J}_1(\boldsymbol{a}) + \boldsymbol{J}_2(\boldsymbol{a}) \tag{12}$$

where, N is the number of the sampling points, t decides the equilibrium between the two parts of the criterion and r_i is a characteristic size of the domain of influence i. The weights w_i ensure the continuity and the locality of the approximation, decreasing within a fixed region around the point i called domain of influence of $\boldsymbol{x}_i$, and vanishing outside.

As described previously, Min($\boldsymbol{J}$) results in the solution of the matrix coefficients $\boldsymbol{a}$ as:

$$\boldsymbol{a}(\boldsymbol{x}) = \mathrm{A}^{-1}\mathrm{B}\boldsymbol{f}, \tag{13}$$

where,

$$\mathrm{A} = \mathrm{PWP}^{T}, \quad \mathrm{B} = \mathrm{PW} \tag{14}$$

$$\mathrm{P} = [\ldots \quad \boldsymbol{p}(\boldsymbol{x}_i - \boldsymbol{x}) \quad \ldots] \tag{15}$$

$$\mathrm{W} = \begin{bmatrix} \boldsymbol{w}(\boldsymbol{x}_1 - \boldsymbol{x}) & & 0 \\ & \ldots & \\ 0 & & \boldsymbol{w}(\boldsymbol{x}_n - \boldsymbol{x}) \end{bmatrix} \tag{16}$$

$$\boldsymbol{w}(\boldsymbol{x}_i - \boldsymbol{x}) = \begin{bmatrix} \mathrm{t}w(\boldsymbol{x}_i - \boldsymbol{x}) & 0 \\ 0 & r^2(1-\mathrm{t})w(\boldsymbol{x}_i - \boldsymbol{x})\mathrm{I}_{n*n} \end{bmatrix} \tag{17}$$

2) EFFICIENCY IMPROVEMENT VIA CUTOFF STRATEGY

To improve the computational efficiency of a MLS based RSM, a cutoff strategy is introduced. The core idea of a cutoff method is that the weighted least-squares procedure formally requires the information from all sampling points. However, the weight function w is highly localized about $\boldsymbol{x}$. Thus, the sampling points far away from $\boldsymbol{x}$ do not significantly influence the least-squares result and can be excluded [14]. This is implemented by adjusting the cutoff radius r_{cut} of the weight function for each sampling point. In other words, the weight function w_i is set to zero if the distance between $\boldsymbol{x}$ and $\boldsymbol{x}_i$, i.e., d_i, is larger than r_{cut}.

In order to assure that $\mathbf{A}$ in (12) and (13) has a full rank, it is necessary that N, the number of sampling points included in the domain of influence of $\boldsymbol{x}_i$, should always be larger than the number of the basis functions M. The simplest approach is that the $r_{\mathrm{cut}}(\boldsymbol{x})$ is set to a fixed large constant [19], resulting in a low computation efficiency and even computation failures. An alternative cutoff method based on the density of data points is to set $r_{\mathrm{cut}}(\boldsymbol{x})$ to be the $(M+1)^{\mathrm{th}}$ smallest $d_i(\boldsymbol{x})$ among the distances of each sampling point $\boldsymbol{x}_{\mathrm{i}}$ from $\boldsymbol{x}$ $\{d_1(\boldsymbol{x}), d_2(x), \ldots, d_{Ntotal}(\boldsymbol{x})\}$, where $Ntotal$ is the number of all sampling points in the whole region of interest [20]. However, when the design problem is a multi-dimensional multimodal problem, this approach may fail when the sampling points are distributed sparsely as demonstrated below. This may be caused by the inconsistency between the number of poles included in the influence domain and the largest number of poles that can be fitted by the basis functions used. Larger number of sampling points may ensure the accuracy of the approximate results, yet sacrifices the computational efficiency especially when the problem in this paper involves several decision variables.

Therefore, a new cutoff method is proposed. The proposed cutoff method decides the cutoff radius based not merely on the density of data points but also on the number of poles roughly estimated in the influence domain to guarantee both sufficient N everywhere and the higher accuracy. That means the cut off criterion of the proposed method includes: first, the number of sampling points included in the domain of influence N is not less than the number of the basis function M; second, the number of the detected poles in the domain of influence $[n_{\mathrm{x}}, n_{\mathrm{y}}, n_{\mathrm{z}}]$ is less than the highest derivative order of the basis function n_{m}.

To give an intuitive explanation of the proposed cutoff method, one takes an example of a three-dimensional [x, y, z] optimization problem. In this three-dimensional problem, the basis function used is: [1, x, y, z, x^2, y^2 z^2, xy, yz, zx], by which the highest derivative order of the objective function can be fitted is 2. The proposed cutoff method is thus explained in Fig. 5.

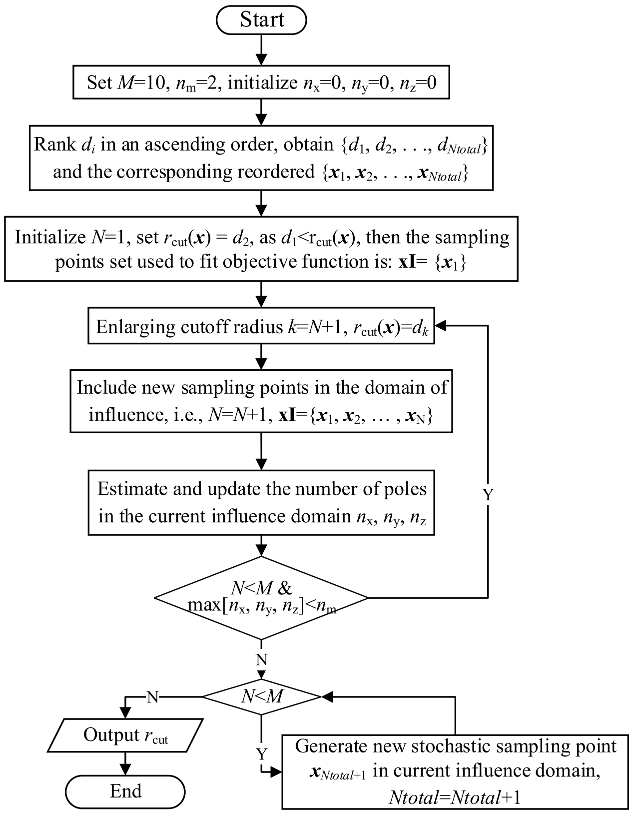

FIGURE 5. The scheme of the proposed cut off method.

To compare the accuracy and validity of the proposed and the original cutoff methods, a mathematic function as given in (17) is reconstructed. There are some key common characteristics between function (17) and the problem to be solved in the paper: both of them are multimodal objective functions, the degree of freedom for both problems is 3 and the highest derivative order of the function for both problems is 2. The approximated results obtained by using the original and the proposed cutoff method are compared in Fig. 6. In the figure, method 1 refers to the original cutoff method, method 2 refers to the proposed cutoff method. Obviously, even for the case that the sampling points are dense enough, the accuracy of the proposed one is still higher than that of the existing one; moreover, as the data points get sparser, the approximated function of the existing cutoff method deviates significantly from the exact one whereas the proposed method still captures the exact values of the original function.

$$f = \mathrm{e}^{-x}\sin(4\pi x)\mathrm{e}^{-y}\sin(4\pi y) + z. \tag{18}$$

C. ADAPTIVE WEIGHTED PARTICLE SWARM OPTIMIZATION ALGORITHM

Particle swarm optimization (PSO) is a population-based heuristic search technique. In a PSO, each particle is treated

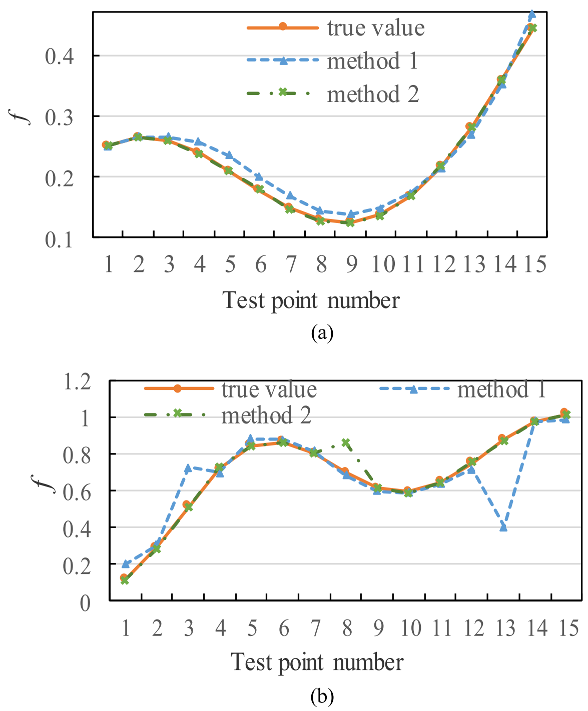

FIGURE 6. **(a) Comparison of the approximated results for dense sampling points; (b) Comparison of the approximated results for sparse sampling points. 'true value' means the exact value from (17).**

as a point in a D-dimensional space and represents a potential solution within the search space, which adjusts its "flying" according to its own flying experience and its companions' flying experience [21]. Each particle has a position vector $\boldsymbol{x}_i$, a velocity vector $\boldsymbol{v}_i$, the position at which the best fitness $\boldsymbol{pbest}_i$ encountered by the particle so far, and the best position of all particles $\boldsymbol{gbest}$ in current generation. The velocity and position updating equations of PSOs are:

$$\boldsymbol{v}_i(t+1) = w\boldsymbol{v}_i(t) + c_1 r_1[\boldsymbol{pbest}_i - \boldsymbol{x}_i(t)] + c_2 r_2[\boldsymbol{gbest} - \boldsymbol{x}_i(t)] \tag{19}$$

$$\boldsymbol{x}_i(t+1) = \boldsymbol{x}_i(t) + \boldsymbol{v}_i(t+1), \tag{20}$$

where c_1 and c_2 are two constants, which are normally taken as 2, r_1 and r_2 are two random numbers, uniformly distributed in [0, 1], w is an inertia weight which controls the influence of the previous velocity: a global search performance is favored with a large inertial weight while a small inertia weight facilitates a local search [22]. In the adaptive weighted particle swarm optimization algorithm (APSO), given a user-specified maximum weight $w_{\max}$ and a minimum weight $w_{\min}$, the inertial weight w is updated as a function of the non-uniformity among fitness values for current particles [23]:

$$w = \begin{cases} w_{\min} - \dfrac{(w_{\max} - w_{\min}) \times (f - f_{\min})}{f_{avg} - f_{\min}}, & f \le f_{avg} \\ w_{\max}, & f > f_{avg}, \end{cases} \tag{21}$$

where f_{avg} and $f_{\min}$ represent the averaged and minimum values of the objective function of all particles respectively.

When the objective function values of all particles tend to be consistent or tend to be local optimal, the inertia weight will increase, while when the objective function values of all particles are dispersed, the inertia weight will be reduced. Meanwhile, for the particle whose objective function value is lower than the average objective function value, the inertia weight factor corresponding to it is larger, which brings the particle closer to a better search area. Therefore, APSO further balances the global search ability and local improvement ability of the PSO algorithm. The detailed algorithm can be described as:

(1) Initialization. Randomly generate n particles $\boldsymbol{x}_i(i = 1, 2, \ldots, n)$, $it_{\max}$ is the maximum iteration number.

(2) Calculate the adaptive degree f. On the basis of adaptive degree, the so-far best position $\boldsymbol{pbest}_i$ for each particle and the so-far best position for the entire swarm $\boldsymbol{gbest}_i$ are calculated.

(3) Generate new particles for the next generation based on (18) - (20).

(4) Check whether the termination criteria are satisfied. The termination criteria are either achieving the forecasting precision or reaching the maximum iteration number. If neither criterion is satisfied, go to Step 2, otherwise, continue to Step 5.

(5) Terminate the searching process and output the results.

IV. NUMERICAL RESULTS AND DISCUSSIONS

For the performance comparison, the prototype hybrid excitation system is optimally designed using both the adaptive weighted particle swarm optimization algorithm (APSO) based on the improved RSM (Improved RSM-APSO) and the original RSM (RSM-APSO) respectively. This problem is also solved directly by using a traditional strategy (APSO), i.e., the computationally optimal problem is directly solved by using the APSO. The final optimized solutions of the prototype hybrid permanent magnet and electrically excited coil system by different methods, together with their performance comparisons, are given in Table 1.

From these numerical results, it is obvious that:

1) the final results obtained by the proposed methodology are nearly the same with those by directly solving the original computationally heavy problem using APSO;

2) the total CPU time used by the proposed methodology is about 59% of that used by APSO;

3) although the original RSM (RSM-APSO) is more computationally efficient than the adaptive weighted particle swarm optimization algorithm (APSO) based on the improved RSM (Improved RSM-APSO), the final solution of the former is far away from that by directly solving the original computationally heavy problem using APSO.

Therefore, the proposed method is more effective and accurate than the original methods in finding optimal solutions.

TABLE 1. Optimized decision parameters.

	H_M (mm)	W_M (mm)	H_C (mm)	W_C (mm)	J_C (A/mm^2)	f	Costed time
RSM-APSO	477	164	600	34	19.36	0.2307	22h 15mins
Improved RSM-APSO	394	163	385	31	19.60	0.1059	26h 31mins
APSO	374	168	370	31	19.27	0.1046	45h

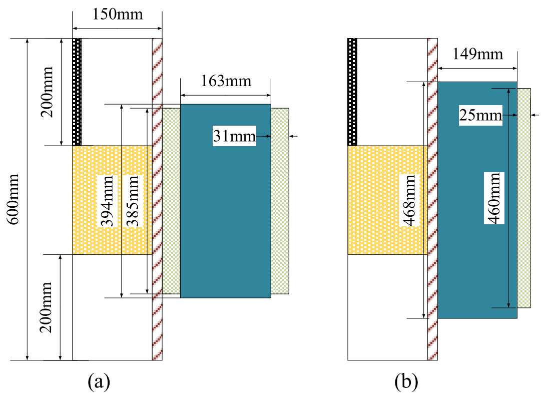

FIGURE 7. (a) The optimized prototype hybrid excitation system with a double coil; (b) The optimized prototype hybrid excitation system with a single coil.

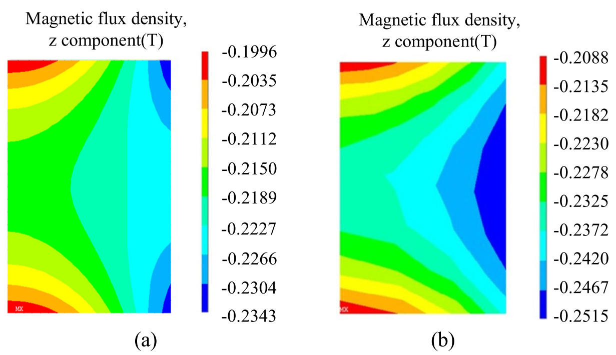

FIGURE 8. The magnetic field in the normal operation condition of the hybrid excitation system: (a) with a double coil; (b) with a single coil.

To support the necessity of using the proposed hybrid excitation system topology, the finally optimized prototype hybrid excitation system with a double coil and that with a single coil are given in Fig. 7 (a) and Fig. 7 (b), respectively. The profiles of the electromagnetic field in the normal operating condition and the arc triggering stage for the two optimized topologies are shown in Fig. 8 and Fig. 9, respectively. Obviously, in the normal operation, the permanent magnet in the excitation systems using both topologies will produce a sufficient strong magnetic field without any aid from the electrically excited field coil to rotate the arc, avoiding the consumption of a great amount of electric energy. However, in the proposed hybrid excitation system with a double coil, the maximum flux density (0.0015T) in the arc triggering stage is nearly zero and

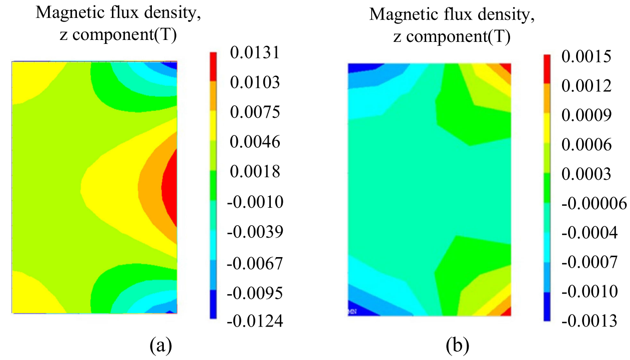

FIGURE 9. The magnetic field in the arc triggering stage of the hybrid excitation system: (a) with a double coil; (b) with a single coil.

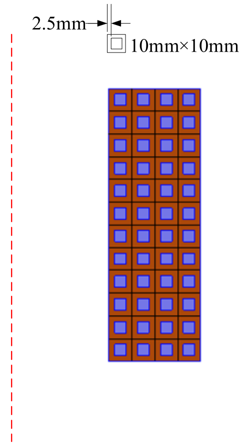

FIGURE 10. The schematic diagram of an electrically excited coil system for the plasma generator.

negligible while that (0.0131) in the hybrid excitation system with a single coil is large enough to prevent an arc from triggering.

To further elaborate the advantages of the proposed system, a traditional water-cooled copper coil excitation system ensuring a minimum magnetic field to be higher than 0.2 T is designed, as is shown in Fig. 9. The electrical resistivity of the copper is $1.667 \times 10^{-8}\Omega$·m and the applied current density is 18 A/mm^2. The electric power consumption of the corresponding excitation system reaches 20 kW, which is quite considerable especially for a long cycle work duty. In contrast, the hybrid excitation system consumes zero electric power to continuously provide the required magnetic field, resulting in a huge amount of energy saving.

Also, to demonstrate the necessity to guarantee a zero magnetic field in arc triggering, one analyzes the physical mechanism of arc triggering. As it is well known, the most popular technique to trigger an arc is breakdown of the dielectrics by a high electric strength. With respect to the proposed plasma generator as schematically given in Fig. 10, to produce an enough strong electric field on the dielectrics, a movable contact (electrically connected with the anode) is

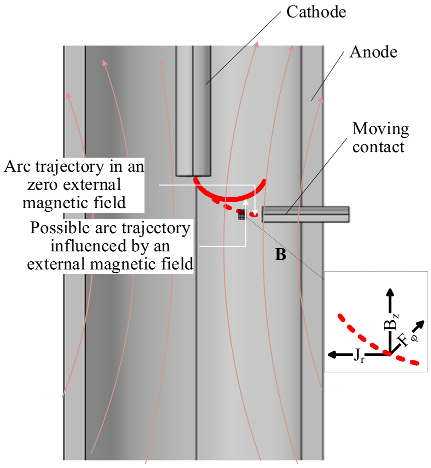

FIGURE 11. Trajectory analysis of the triggered arc.

introduced in the generator. To provide an enough electric field on the dielectrics to make it breakdown to form an arc, the movable contact will approach the cathode as close as possible at the beginning of the arc triggering, gradually and smoothly return back to the anode to finalize the arc triggering, as illustrated in Fig. 10. However, if there is an external magnetic field in the arc triggering region, the tangential Lorentz force generated by the interaction between the radial component of current and the axial component of magnetic field forces the arc to rotate. As a result, the arc end cannot pinpoint to the movable contact, resulting in an arc triggering failure.

V. CONCLUSION

A novel topology of a hybrid permanent magnet and electrically excited coil system for a coaxial dc arc plasma generator is proposed and optimized in this paper. The numerical results of an optimized prototype hybrid excitation system have demonstrated that the proposed hybrid excitation system covers the advantages of both a permanent magnet and an electrically excited coil system. The system comprehensively considers factors including the material cost, the system performance and the influence of permanent magnet on arc triggering. It realizes energy saving during normal operation and successful arc striking during arc striking, allows the generated magnetic field to be easily adjusted due to the flexible adjustability of the coil current and has excellent technical and economic performance. Consequently, the proposed hybrid excitation system is promising in engineering applications. On the other hand, for excitation systems with complex structure, the improved optimization method significantly improves the optimization efficiency of the device on the premise of completing the design requirements. The proposed approach is also efficient in solving other optimal problems in which the objective function is determined by computationally heavy approaches such as the 2-D or 3-D FE analysis.

REFERENCES

[1] J. R. Roth, "DC electrical arc discharges in gases," in *Industrial Plasma Engineering: Principles*, vol. 1. Boca Raton, FL, USA: CRC Press, 1995, ch. 10, sec. 7, pp. 401–402.
[2] V. Nemchinsky, "Modeling arc in transverse magnetic field by using minimum principle," *IEEE Trans. Plasma Sci.*, vol. 44, no. 11, pp. 2932–2935, Nov. 2016, doi: 10.1109/TPS.2016.2616099.
[3] V. Nemchinsky, "A method to reduce electrode erosion in a magnetically driven rotating arc," *IEEE Trans. Plasma Sci.*, vol. 44, no. 12, pp. 3474–3478, Dec. 2016, doi: 10.1109/TPS.2016.2628885.
[4] C. Wang, M. Song, X. Chen, D. Li, and W. Xia, "Synthesis of few-layer graphene flakes by magnetically rotating arc plasma: Effects of input power and feedstock injection position," *Appl. Phys. A, Solids Surf.*, vol. 126, no. 3, pp. 1–13, Feb. 2020, doi: 10.1007/s00339-020-3399-6.
[5] C. Wang, J. Zhou, M. Song, Z. Lu, X. Chen, Y. Zheng, and W. Xia, "Synthesis of ultrafine silicon carbide nanoparticles using nonthermal arc plasma at atmospheric pressure," *J. Amer. Ceram. Soc.*, vol. 104, pp. 3883–3894, Mar. 2021, doi: 10.1111/jace.17811.
[6] C. Wang, Q. Sun, L. Sun, W. Xia, and W. Xia, "Spot and diffuse mode of cathode attachments in a magnetically rotating arc plasma generator at atmospheric pressure," *J. Appl. Phys.*, vol. 125, no. 3, Jan. 2019, Art. no. 033301, doi: 10.1063/1.5081113.
[7] M. Zhang, J. Ma, G. Wen, Q. Yang, B. Su, and Q. Ren, "Gas production from polyethylene terephthalate using rotating arc plasma," *Chem. Eng. Process. Process Intensification*, vol. 128, pp. 257–262, Jun. 2018, doi: 10.1016/j.cep.2018.04.021.
[8] V. Nemchinsky, "A 'resonance' method to decrease electrode erosion in magnetically rotated arcs," *IEEE Trans. Plasma Sci.*, vol. 47, no. 1, pp. 742–745, Jan. 2019, doi: 10.1109/TPS.2018.2863251.
[9] H. Wu, Y. Chang, L. Lu, and J. Bai, "Review on magnetically controlled arc welding process," *Int. J. Adv. Manuf. Technol.*, vol. 91, pp. 4263–4273, Feb. 2017, doi: 10.1007/s00170-017-0068-9.
[10] H. Zhang, L. I. Xiaodong, and Z. H. Yunqing, "Experimental research of hydrogen production from methane reforming in nitrogen using a rotating gliding arc reactor," *J. Eng. Thermophys.*, vol. 34, no. 4, pp. 787–790, 2013.
[11] J. Robinson and Y. Rahmat-Samii, "Particle swarm optimization in electromagnetics," *IEEE Trans. Antennas Propag.*, vol. 52, no. 2, pp. 397–407, Feb. 2004, doi: 10.1109/TAP.2004.823969.
[12] F. Han, W.-T. Chen, Q.-H. Ling, and H. Han, "Multi-objective particle swarm optimization with adaptive strategies for feature selection," *Swarm Evol. Comput.*, vol. 62, Apr. 2021, Art. no. 100847, doi: 10.1016/j.swevo.2021.100847.
[13] M. Mahfouf, M. Y. Chen, and D. A. Linkens, "Adaptive weighted particle swarm optimisation for multi-objective optimal design of alloy steels," in *Proc. PPSN*, Birmingham, U.K., 2004, pp. 762–771.
[14] P. Breitkopf, H. Naceur, A. Rassineux, and P. Villon, "Moving least squares response surface approximation: Formulation and metal forming applications," *Comput. Struct.*, vol. 83, pp. 1411–1428, Jun. 2005.
[15] K. Anjneya and K. Roy, "Response surface-based structural damage identification using dynamic responses," *Structures*, vol. 29, pp. 1047–1058, Feb. 2021, doi: 10.1016/j.istruc.2020.11.033.
[16] R. H. Myers, D. C. Montgomery, and C. M. Anderson-Cook, "The analysis of second-order response surfaces," in *Response Surface Methodology: Process and Product Optimization Using Designed Experiments*, 4th ed. Hoboken, NJ, USA: Wiley, 2016, pp. 273–325.
[17] P. Lancaster and Š. Kęstutis, "Moving least squares and composite methods," in *Curve and Surface Fitting: An Introduction*. London, U.K.: Academic, 1986, ch. 10, pp. 225–244.
[18] P. Joyot, F. Chinesta, P. Villon, and B. Khoshnoudirad, "Hermite MLS approximation for discretizing fourth order partial differential equations encountered in beam and plate models," *AIP Conf. Proc.*, vol. 907, no. 1, pp. 1384–1389, 2007.
[19] X. Li and S. Li, "Analysis of the complex moving least squares approximation and the associated element-free Galerkin method," *Appl. Math. Model.*, vol. 47, pp. 45–62, Jul. 2017, doi: 10.1016/j.apm.2017.03.019.
[20] M. Matinfar and M. Pourabd, "Modified moving least squares method for two-dimensional linear and nonlinear systems of integral equations," *Comput. Appl. Math.*, vol. 37, pp. 5857–5875, Jun. 2018, doi: 10.1007/s40314-018-0667-6.
[21] Y. Shi and R. C. Eberhart, "Parameter selection in particle swarm optimization," in *Evolutionary Programming VII*. Berlin, Germany: Springer, 1998, pp. 591–600.

[22] D. Chen and C. Zhao, "Particle swarm optimization with adaptive population size and its application," *Appl. Soft Comput.*, vol. 9, no. 1, pp. 39–48, Jan. 2009, doi: 10.1016/j.asoc.2008.03.001.
[23] C. Gong and Z. Wang, *Proficient in MATLAB Optimization Calculation*. Beijing, China: Electronic Industry Press, 2009, pp. 280–295.

XIAOWEN XU was born in Jinhua, Zhejiang, China, in 1994. She received the B.S. degree in electrical engineering from North China Electric Power University, China, in 2016. She is currently pursuing the Ph.D. degree in electrical engineering with Zhejiang University, Hangzhou, China. From 2019 to 2020, she was a Joint Supervision Ph.D. Student with Sorbonne University. Her research interests include multi-physics modeling and simulation of plasma, numerical analysis, and optimization of engineering electromagnetic field.

ZHUOXIANG REN (Senior Member, IEEE) received the B.S. degree from the Huazhong University of Science and Technology, Wuhan, China, in 1982, and the Ph.D. degree in electrical engineering from the Insititut National Polytechnique de Toulouse, Toulouse, France, in 1986.

He was an Assistant Professor with the Ecole Normale Superieure de Cachan; a Senior Researcher with the Laboratoire de Genie Electrique de Paris, Centre Nationale de Recherche Scientifique, Paris; a Visiting Professor with The University of Akron, Akron, OH, USA; a Guest Professor with the Chinese Academy of Sciences; and a Staff Engineer or a Principal Engineer with various EDA companies, including Ansoft Corporation, Pittsburgh, PA, USA; Cadence Design Systems Inc., San Jose, CA, USA; and Mentor Graphics Corporation, Wilsonville, OR, USA. He is currently a Professor with Sorbonne Universités, Université Pierre et Marie Curie–Paris 6, Paris, France, and serves as the Group Leader in micro and nanoelectronics with the Laboratory of Electronics and Electromagnetism. He has authored over 140 refereed journal and international conference papers, and coauthored two book chapters. His current research interests include numerical methods for the computation of electromagnetic fields, modeling and extraction of micro and nanoscale interconnects and devices, and modeling and simulation of microelectronic systems. He received the Bronze Medal of CNRS in France, in 1996.

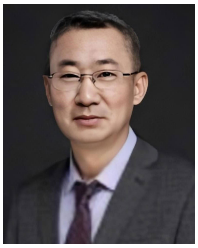

SHIYOU YANG (Senior Member, IEEE) was born in Liaoning, China, in 1965. He received the M.S. and Ph.D. degrees in electrical engineering from the Shenyang University of Technology, Liaoning, in 1990 and 1995, respectively.

He has been a Full Professor with the College of Electrical Engineering, Zhejiang University, China, since 2001. He has worked with the Department of Electrical and Computer Engineering, Duke University, USA, from November 2007 to May 2008, as a Visiting Scholar; and Université Pierre et Marie Curie, France, from September 2017 to October 2017, as a Visiting Professor. So far, he has published more than 150 papers in refereed international conference and journals, and more than 100 in high-rank international journals. His research interests include engineering electromagnetics and application, computational electromagnetics in both high and low frequency domains, and numerical methodology for direct and inverse problems, including multi-physics field computations. He is a Board Member of COMPUMAG and a member of the International Steering Committee of IEEE CEFC and the International Steering Committee of the International Symposium on Applied Electromagnetics and Mechanics (ISEM).